Design Options for Thermal Shutdown Circuitry with Hysteresis Width Independent on the Activation Temperature

Cosmin-Sorin PLESA[1], Marius NEAG[1], Liviu RADOIAS[2]
[1]*Technical University of Cluj-Napoca, Basis of Electronics Department, 400027, Romania*
[2]*INFINEON Technologies, Munchen, Germany*
Cosmin.Plesa@bel.utcluj.ro

***Abstract*—This paper presents several design options for implementing a thermal shutdown circuit with hysteretic characteristic, which has two special features: a programmable activation temperature (the upper trip point of the characteristic) and a hysteresis width largely insensitive to the actual value of the activation temperature and to variations of the supply voltage. A fairly straightforward architecture is employed, with the hysteresis implemented by a current source enabled by the output of the circuit. Four possible designs are considered for this current source: VBE/R, modified-VBE/R, Widlar and a peaking current source tailored for this circuit. First, a detailed analytical analysis of the circuit implemented with these current sources is performed; it indicates the one best suited for this application and provides key sizing equations. Next, the chosen current source is employed to design the thermal shutdown protection of an integrated Low-Dropout Voltage Regulator (LDO) for automotive applications. Simulation results and measurements performed on the silicon implementation fully validate the design. Moreover, they compare favorably with the performance of similar circuits reported recently.**

***Index Terms*—bipolar integrated circuits, hysteresis, integrated circuit reliability, power system protection, thermal analysis.**

I. INTRODUCTION

Thermal shutdown is a basic feature of modern integrated circuits (ICs) with substantial power dissipation, such as power amplifiers and voltage regulators [1-3], in order to prevent possible overheating that can lead to irreversible damage due, for example, to transistors breakdown at high temperatures [4]. Thermal phenomena in integrated circuits are complex and could affect the IC robustness [5-6] but with a proper thermal shutdown circuitry the long-term reliability can be ensured. In general, the thermal shutdown circuitry comprises a temperature monitor, which changes the voltage or current level at its output when the die temperature reaches a set threshold value and execution elements triggered by the monitor, able to change the operating condition of the protected circuit or system, limiting its power dissipation until the over-temperature condition disappears.

If the temperature monitor operates as a simple comparator the system can engage itself in repetitive on-off cycles. An effective solution is to implement a hysteresis in the temperature-output voltage or current characteristic of the thermal shutdown circuit. Thus, the upper threshold of the hysteresis should be set high enough so that the protection is not activated during the normal operating of the system, while the hysteresis should be wide enough to prevent thermal oscillations near the activation temperature threshold.

A typical implementation of the thermal monitor is based on a simple voltage comparator: a temperature-independent voltage, V_{REF}, usually provided by a bandgap voltage reference, is applied at one input, while a temperature-dependent voltage is applied to the other input of the comparator [7]. Several other approaches have been proposed in the literature, the one proposed in [8] implements a nonlinear current modifier to detect the over-temperature condition, which results in the disabling of the biasing of the protected circuit. Another approach is to compare a compensated current derived from a bandgap voltage reference with a temperature dependent current in order to trigger the activation temperature of the thermal shutdown protection [9].

Two common issues that hinder the performance of numerous thermal shutdown circuits proposed so far are: lack of accuracy in setting the trip point (or points for those with a hysteretic characteristic) and large sensitivity to supply voltage variations [10-11]. These issues are addressed by the thermal shutdown circuit proposed in this paper. In particular, it features a hysteretic characteristic, with the hysteresis width largely insensitive to supply voltage variation (within the range 4.5V+/-1V); the temperature range is -40°C to +180°C.

Additional features are demanded by applications with tough reliability requirements, as is the case for automotive ICs. On one hand, one needs to perform extended tests in order to ensure the product quality while on the other hand the costs should be maintained at reasonable levels [12]. A standard solution is to induce accelerated ageing by over-stressing the IC in order to test quicker their reliability. For example, the High-Temperature Operating Life (HTOL) test implies running the IC at junction temperatures higher than their normal operating range [13-14]; for this, the thermal shutdown circuit should allow for programmable activation temperature. Furthermore, the width of the hysteresis should not change when the activation temperature changes and should be largely insensitive to supply variations. To the authors' best knowledge these points have not yet been

This work was co-funded by Infineon Technologies Romania and the Operational Program "Competitiveness" POC -A1.2.3-G-2015, through the project "PartEnerIC", P_40_437.

Digital Object Identifier 10.4316/AECE.2017.01010

addressed in the open literature.

Several circuit implementations for a thermal shutdown circuitry endowed with all the features mentioned above are proposed and analyzed comparatively in this paper.

Section II starts with a general description of the proposed architecture that employs a current source controlled by the output of the circuit in order to realize the hysteretic characteristic. Next, three possible circuit implementations based on well-known current sources are analyzed. Finally, the proposed circuit is introduced, which overcomes the short comings of the standard solutions by using a modified peaking current source. Section III presents simulation results and measurements performed on a silicon implementation of the proposed circuit; they demonstrate the advantages of this new thermal shutdown circuit. The main results and conclusions are summarized in the last Section.

II. Proposed Thermal Shutdown Circuitry

A. General description of the architecture

The block diagram of the thermal shutdown circuit described in this paper is presented in Fig. 1. It is somewhat similar to the circuit proposed in [9]: it employs a voltage comparator to monitor the difference between a temperature-independent reference voltage, V_{REF}, and a voltage with a complementary-to-absolute-temperature variation, V_{NTC}, generated by a bipolar transistor. The circuit is sized so that in normal operation the voltage V_{NTC} is higher than V_{REF}. When the die temperature increases the value of the V_{NTC} voltage decreases, so that at a certain temperature it becomes smaller than V_{REF}, causing the comparator to trip, thus turning on transistor T1. In turn, this enables a current source with two outputs: the first output injects a current into resistor R_1, thus pushing up the voltage level at the node TSD_{OUT}. Finally, the output voltage, V_{OUT}, goes high and this flag activates the circuitry within the system (not shown here) that changes the operating condition of the protected circuit. The comparator trip condition is given by:

$$V_{TRIP1} = V_{REF} \tag{1}$$

The second output of the current source enabled by T1 injects the current I_{HYST} into the resistor R_4, part of the resistor ladder employed to derive the reference voltage, V_{REF}. Thus, the trip condition of the comparator changes to:

$$V_{TRIP2} = V_{TRIP1} + I_{HYST} \cdot R_4 \tag{2}$$

Therefore, the thermal shutdown circuitry will be de-activated at a lower temperature than the one that activates it, given by (1), that is a hysteresis is realized. Its width is set by the current I_{HYST} provided by the current source:

$$\Delta H[V] = I_{HYST} \cdot R_4 \tag{3}$$

For the circuit implementation of Fig. 1, resistors R_2 and R_3 are replaced by a resistive ladder with multiple tap points; thus, one can program digitally V_{TRIP1} – and thus the activation temperature – by simply choosing which tap point is connected to the noninverting input of the OA. Similarly, the width of the hysteresis is made programmable by implementing the current source cell as a current mirror with adjustable gain for its IHYST output.

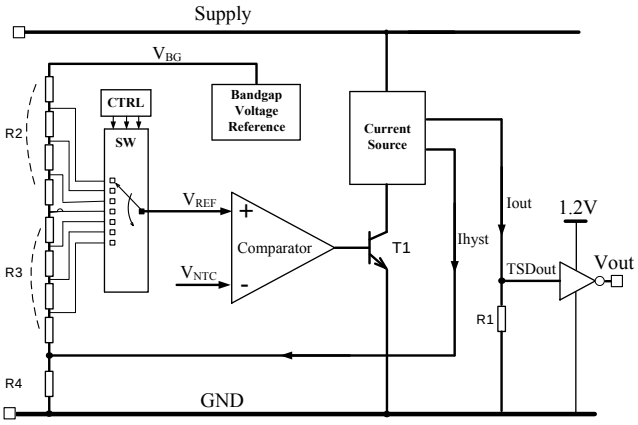

Figure 1. Block Diagram of the Thermal Shutdown Circuitry with hysteretic characteristic implemented by the current

It is apparent that the current source is a key element of this architecture, as its accuracy and sensitivity to supply variations determines the precision the second trip point can be set by. The temperature variation of the hysteresis current will impact the hysteresis width for different activation temperature of the thermal protection.

In the followings we analyze comparatively four possible circuit implementations of this current source.

B. Standard solutions for implementing the current source

Fig. 2 presents three possible implementations of the "**Current Source**" cell in the block diagram shown in Fig. 1, based on fairly standard circuits. For the modified-V_{BE}/R current source shown in Fig. 2(a) a simple expression for the output current can be obtained by neglecting the saturation voltage of T1, used here as an on/off switch (V_{CEsat1} = 0V):

$$I_{HYST} = \frac{V_{SUPPLY} - V_{EB2}}{R_2} - \frac{V_{EB2}}{R_1} = \frac{V_{SUPPLY}}{R_2} - V_{EB2}\left(\frac{1}{R_1} + \frac{1}{R_2}\right) \tag{4}$$

Equation (4) indicates that for this implementation the second trip point, V_{TRIP2}, and the hysteresis width, ΔH, depend linearly on both, the supply voltage, V_{SUPPLY}, and temperature. Their proportional to absolute temperature (PTAT) variation is apparent due to the negative factor the base-emitter voltage V_{BE2} is multiplied by. Note that the thermal behavior of the resistances has not been taken into consideration here.

The Widlar current source shown in Fig. 2(b) is usually employed to generate small currents without resorting to large resistors. Assuming that for transistors T2 and T3 the collector currents have much larger values than their saturation currents, one can write the following equation:

$$I_{HYST} = \frac{V_T}{R_1} \ln \frac{I_{IN}}{I_{HYST}} \tag{5}$$

By assuming again that V_{CEsat1} = 0V the current I_{IN} results:

$$I_{IN} = \frac{V_{SUPPLY} - V_{EB2}}{R_2} \tag{6}$$

The expression of the current provided by the VBE/R current source shown in Fig. 2(c) [15] is not surprisingly:

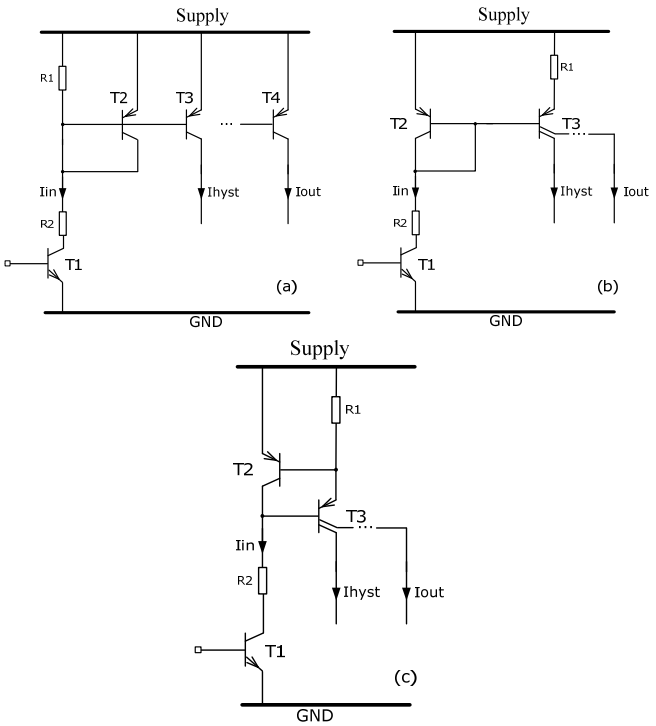

Figure 2. Three possible implementations of the "Current Source" block shown in Fig.1: (a) Modified-V_{BE}/R current Source (b) Widlar current source and (c) V_{BE}/R current Source [8]

$$I_{HYST} = \frac{V_{EB2}}{R_1} \tag{7}$$

It follows that this current has a CTAT (Complementary to Absolute Temperature) variation with temperature, determined by the base-emitter voltage of the transistor T2.

It will be shown later that of the three circuits shown in Fig. 2 the Widlar current source provides the smallest variations of I_{HYST} over the temperature and voltage supply ranges envisaged here. The modified-V_{BE}/R source provides the second smallest temperature variation while the variation with the voltage supply of the V_{BE}/R source is comparable with the variation of Widlar current source.

C. Improved solution based on the peaking current source

A better solution for implementing the "**Current Source**" cell within the thermal shutdown block diagram shown in Fig. 1 is the peaking current source presented in Fig. 3. It was derived from the NPN current source proposed in [16-17], designed so that the sensitivity of its output currents to both temperature and process variations was minimized. The resistor R_1 was added for two reasons: i) to ensure the current source remains off when T_1 is off, even in the presence of large leakage currents and ii) it provides an additional design variable for minimizing the temperature variation of I_{HYST}.

The output currents can be expressed as a function of the emitter-base voltage of T_3, such as:

$$I_{HYST} = I_{S3} \cdot e^{\frac{q \cdot V_{EB3}}{K \cdot T}} \tag{8}$$

where q, K, T are the electron charge, Boltzmann constant and absolute temperature, respectively, while I_{S3} is the saturation current of transistor T_3. By ignoring the base currents, the expression for the emitter-base voltage of transistor T_3 can be written simply as:

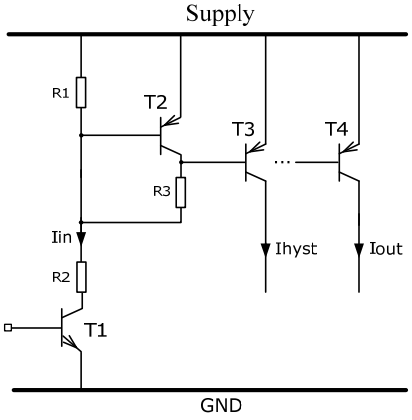

Figure 3. The peaking current source proposed here for implementing the "Current Source" block shown in Figure 1.

$$V_{EB3} = V_{EB2} - I_{R3} \cdot R_3 = \frac{K \cdot T}{q} \cdot \ln \frac{I_{R3}}{I_{S2}} - I_{R3} \cdot R_3 \tag{9}$$

The current through R_3, I_{R3}, depends on the supply voltage:

$$I_{R3} = I_{IN} - I_{R2} = \frac{V_{SUPPLY} - V_{EB2}}{R_2} - \frac{V_{EB2}}{R_1} \tag{10}$$

but from (9) and (10) one can derive an optimum value for resistor R_3, for which the variations of I_{R3} do not affect the emitter-base voltage of T_3:

$$\frac{\partial V_{EB3}}{\partial I_{R3}} = 0 \rightarrow R_{3optim} = \frac{K \cdot T}{q} \cdot \frac{1}{I_{R3}} \tag{11}$$

Obviously, equation (11) cannot be fulfilled for all temperature and voltage supply values but the designer can size R_3 considering the nominal values for the temperature and supply voltage. It will be shown that with this value, called here R_{30}, the variation over the voltage supply range envisaged here of the currents provided by this source can be made smaller than for the Widlar current source shown in Fig. 2(b).

Let us now analyze the temperature dependency of the hysteresis width, under the same conditions (R_3=R_{30} and I_{S2}=I_{S3} and considering the usual, first-order, thermal variations for resistors: $R = R_0[1 + \alpha(T - T_0)]$ where α is the resistor temperature coefficient (TC) - and base-emitter voltages: $V_{BE} = V_{BE0} + \lambda(T - T_0)$, where λ is the base-emitter TC (-2mV/°C typically). The relative variation of $\Delta H[V]$ with temperature can be approximated as follows:

$$\frac{\partial \Delta H[V]}{\Delta H[V]} \cdot \frac{1}{\partial T} = \frac{\lambda}{\Delta I_{IN}} + \left(1 + \frac{\lambda(T - T_0)}{\Delta I_{IN}} \cdot \left(\frac{q \cdot \lambda}{K \cdot T} - \frac{q \cdot \Delta I_{IN} + \lambda(T - T_0)}{K \cdot T^2}\right) \cdot \frac{R_{30}}{R_{20}}\right) \tag{12}$$

where ΔI_{IN} is the variation with temperature of the input current, I_{IN}, as given by first term of (10). It is worth noting that the effects of temperature variation of resistors R_3 and R_2 cancel each other, if these resistors have the same TC.

Equation (12) indicates that the temperature variation of ΔH can be minimized if the ratio between resistors R_3 and R_1 has an "optimum" value, given by the following expression:

$$\left(\frac{R_3}{R_1}\right)_{OPTIM} = \frac{K \cdot \lambda \cdot T_0}{q \cdot \Delta I_{IN} \cdot \left(\frac{\Delta I_{IN}}{T_0} - \lambda\right)} \tag{13}$$

This can be used as a sizing equation similarly to (11).

Therefore this design option offers the possibility to

obtain a current quite stable with temperature and this will result, as can be seen in (4), in a hysteresis width insensitive with the temperature variation which could be the case when you have different activation temperature thresholds for the thermal protection.

III. Design Example: Thermal Shutdown Circuit Integrated Within An Automotive LDO

The circuits presented in the previous section were considered for implementing the thermal shutdown protection of an integrated LDO for automotive application. The following design requirements were set:

- activation temperature (corresponding to V_{TRIP1}): T_{HIGH}= 180°C+/-10%;
- hysteresis width ΔH[°C]: 15°C+/-10%;
- range of supply voltage: V_{SUPPLY} = 4.5V +/-1V.
- operating temperature range: -40°C to +200°C

Starting with the block diagram shown Fig. 1, the fourth possible implementation of the "**Current Source**" cell there, presented in Fig. 2 and Fig. 3, were sized based on the analytical analysis presented in Section II. Fig. 4 and Fig. 5 show the simulated variation of the output currents of the resulting current sources over the temperature and supply ranges considered here; they confirm the analytical analysis.

Fig. 4 shows that the output current yielded by the peaking current source shown in Fig. 3, sized by using (11) and (13) has the smallest temperature variation: its value varies by less than 5% over the temperature range 100°C to 180°C. The currents generated by both the Widlar and the modified-V_{BE}/R sources have a PTAT behavior, resulting in far larger variations of their values over the same temperature range: 21% for the Widlar current source and 32% for the modified-V_{BE}/R source. The current generated by the V_{BE}/R source has a CTAT behavior, exhibiting the largest variation over the 100°C to 180°C temperature range, of about 40%.

The peaking current source is also the best in respect to sensitivity to supply variations, but by smaller margins: its output current varies by 5% around the nominal value of 1.25 uA when V_{SUPPLY} varies between 3.5V to 5.5V, while the currents provided by the Widlar and V_{BE}/R sources vary by about 15%. Under the same conditions the modified-V_{BE} current source has the largest variation, 64%.

Based on the temperature variation illustrated in Fig. 6 one can convert the hysteresis width expressed by (3) in volts, ΔH[V], to a hysteresis width expressed in degrees Celsius, ΔH[°C]. The variation of the V_{NTC} when the temperature varies between 100°C and 180°C is approximately 160mV, so the average slope of the V_{NTC} versus temperature characteristic is -2mV/°C.

Fig. 6 presents the temperature variation of the two voltages applied to the inputs of the comparator shown in Fig. 1: one notices that, as predicted by (2), the reference voltage increases once the activation temperature, T_{HIGH} =180°C, is reached.

In order to prove that the hysteresis width of the chosen circuit (with the architecture shown in Fig. 1 and the "Current Source" cell there implemented by the peaking current source shown in Fig. 3) is insensitive to the value of activation temperature we performed two sets of simulations, setting the activation point to 185°C and 165°C, respectively.

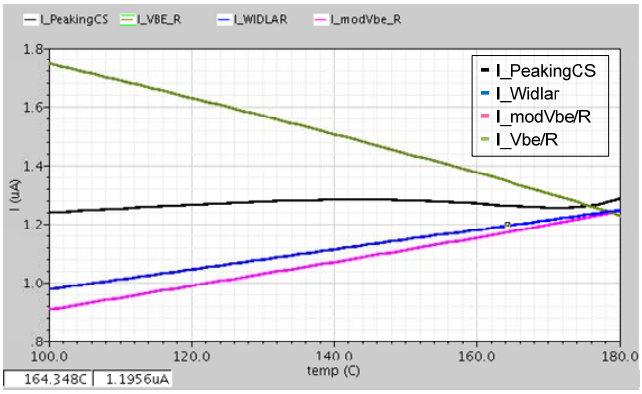

Figure 4. Temperature variation of the currents generated by the four sources considered for implementing the "Current Source" block shown in Fig. 1.

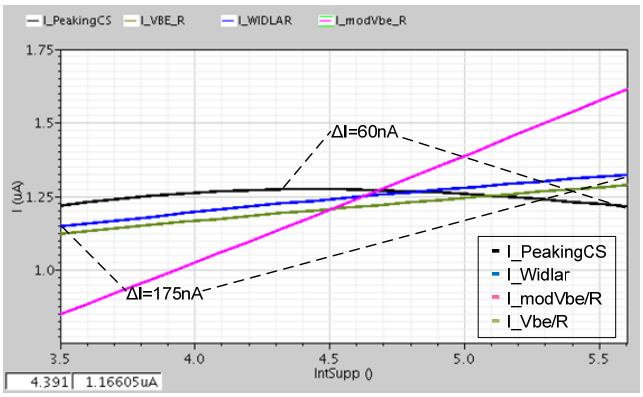

Figure 5. Effect of voltage supply varying between 3.5V and 5.5V over the current generated by the four sources considered for implementing the "Current Source" block shown in Fig. 1.

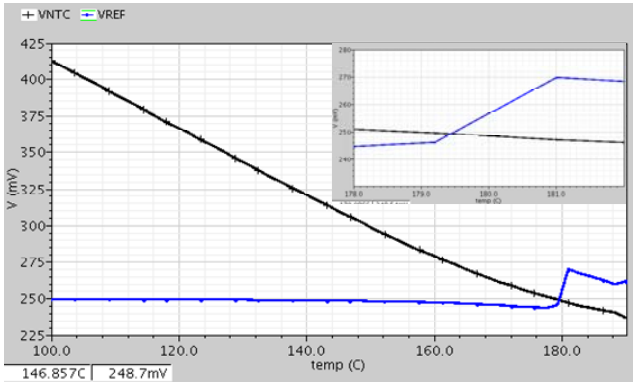

Figure 6. Temperature variation of the two voltages applied to the inputs of the comparator shown in Fig. 1. The fact that V_{REF} jumps when the activation temperature is reached demonstrates the hysteretic characteristic.

The results are shown in Fig. 7: first, the junction temperature was gradually increased from 140°C to 190°C, and the output voltage of the circuits was monitored. Initially, it had a "High" value (1.2V) but when the width is 15°C in both cases (Fig. 7 top and bottom, respectively) proving that ΔH[°C] does not vary significantly with the value of the activation temperature. Next, the temperature was decreased gradually from 190°C to 140°C and the deactivation temperature was obtained. One can see that the hysteresis width is 15°C in both cases (Figure 7 top and bottom, respectively) proving that ΔH[°C] does not vary significantly with the value of the activation temperature.

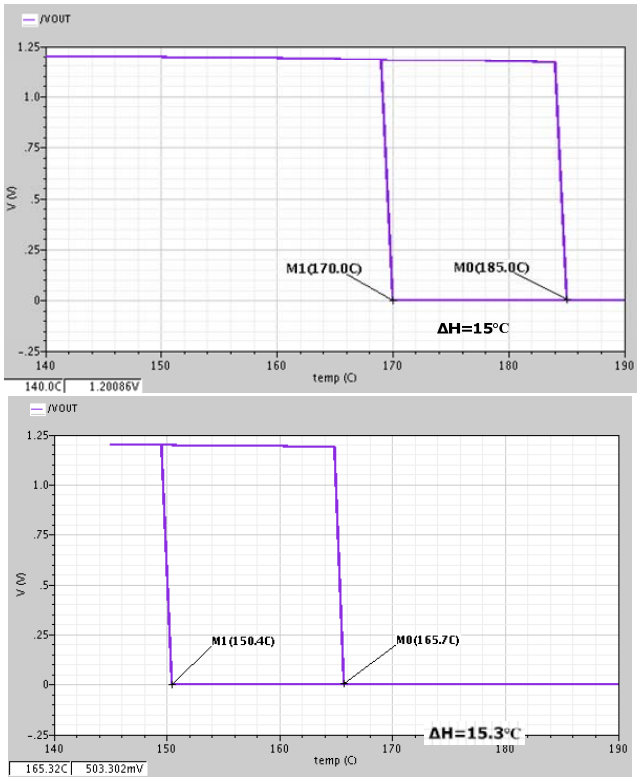

Figure 7. Simulation result for the circuit shown in Fig. 1 with the activation temperature set to 185°C (top) and 165°C (bottom).

TABLE I. SUMMARY OF THE HYSTERESIS WIDTH VALUES, ΔH, FOR ALL FOURTH SOURCES USED FOR THE "CURRENT SOURCE" BLOCK SHOWN IN FIG. 1

Current Source Type	Hysteresis Width [°C]			
	Supply=3.5V		Supply=5.5V	
	T_{HIGH} set to 165°C	T_{HIGH} set to 185°C	T_{HIGH} set to 165°C	T_{HIGH} set to 185°C
Peaking Current Source	14.9	15.1	15	15.3
Widlar Current Source	14.3	14.9	15.5	16.2
Modified - V_{BE}/R Current Source	11.2	13.8	17.1	19.2
V_{BE}/R Current Source	14.4	12.5	15.8	14.8

These results were compared to those yielded by the other design options considered here. For a fair comparison, the thermal shutdown circuits implemented with the current sources shown in Fig. 2 were the sized so that they met the same requirements (the ones listed at the beginning of this Section) and the same tests were performed on them.

The results are summarized in Table I. They are very much in line with the expectations set by Fig. 4 and Fig. 5:

- overall, the trip points vary the least when the peaking current source is employed; the second-best results are provided by the Widlar current source while the modified V_{BE}/R performs the worst.
- this hierarchy is maintained even if one considers only the variation with the activation temperature
- the NTAT behavior of the V_{BE}/R can be observed: for a higher activation temperature the hysteresis width is smaller

Table II presents the variation of the hysteresis width due to component mismatches, obtained by performing Monte-Carlo (MC) analysis on the circuit shown in Fig. 1 implemented with the four current sources considered here. The mean value of ΔH[°C] is practically the same, around 15.5°C, but the standard deviation is far smaller for the peaking current source: 1.71°C compared to 2.02°C, 2.87°C and 3.79°C for the V_{BE}/R, Widlar, and modified-V_{BE}/R current sources, respectively.

TABLE II. VARIATION OF HYSTERESIS WIDTH, ΔH, DUE TO COMPONENT MISMATCH WHEN THE "CURRENT SOURCE" BLOCK SHOWN IN FIG. 1 IS IMPLEMENTED BY THE FOUR SOURCES CONSIDERED HERE

Current Source Type	Mean Value, μ [°C]	Sigma, σ [°C]
Peaking Current Source	15.41	**1.71**
Widlar Current Source	15.49	2.87
Modified - V_{BE}/R Current Source	15.56	3.79
V_{BE}/R Current Source	15.1	2.02

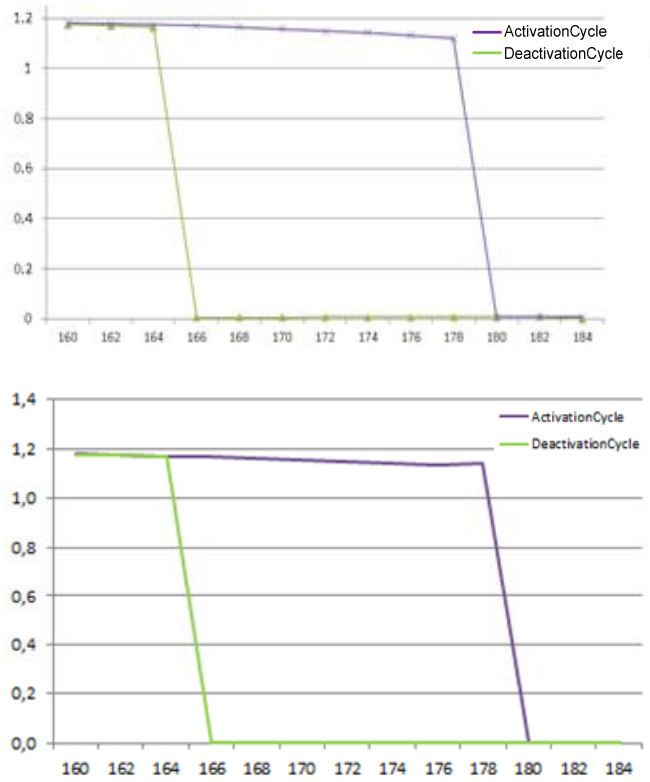

Figure 8. Measured results obtained for a complete activation-deactivation cycle that is, varying the die temperature from 160ºC to 184ºC, then back. Top: V_{SUPPLY}=5.5V; Bottom: V_{SUPPLY}=3.5V

Based on all these results the peaking current source presented in Fig. 3 was chosen for the silicon implementation of the thermal shutdown circuit.

Measurements performed on the silicon implementation of the chosen circuit yielded characteristics that closely matched those shown in Fig. 7, with the differences well within the value of the temperature step, 2°C. Fig. 8 presents two characterisitcs obtained by performing measurements on a similar setup, for two values of the supply voltage: V_{SUPPLY}=5.5V and 3.5V. In both cases the activation temperature was set to 180°C.

The measured values for the activation and deactivation temperatures were +180°C and +166°C, respectively; no variations due to the supply voltage were detected, so one can conclude that those variations were smaller than the step the temperature was varied by, i.e. 2°C. Obviously, this conclusion can be extended to the variation (rather, the lack of) of the hysteresis width with the supply voltage.

Table III presents the main features of the integrated thermal shutdown circuit described in this paper and of two similar circuits proposed in the literature. This allows for a direct comparison, which highlights the advantages of the proposed circuit: programmable activation temperature and hysteresis width largely insensitive to variation of the supply voltage and to the actual value of the activation temperature.

TABLE III. COMPARISON WITH OTHER REFERENCES

	Supply Range [V]	**Activation temp, T_{HIGH} [°C]**	**ΔH value [°C]**	**ΔH varies with T_{HIGH}**	**ΔH varies with V_{SUPPLY}**
Zhang [7]	2 – 12[a]	158	29	Yes	N/A[a]
Tan [9]	3 - 5	150	20	Yes	small
This work	3.5 - 5.5	180[b]	15	No	very small

Note a: Employs a shunt regulator to remove the variation of the supply voltage actually applied to the thermal shutdown circuit

Note b: Programmable between 165°C and 185°C

Of the two references chosen for comparison the circuit proposed in [9] performs the best, but it works over a narrower supply range than the proposed circuit and the width of its hysteresis varies significantly with the activation temperature value.

IV. CONCLUSIONS

This paper presents design options for implementing a thermal shutdown circuit with hysteretic characteristic, which has two features not provided by similar circuits reported in the literature: a programmable activation temperature and a hysteresis width largely insensitive to the actual value of the activation temperature and to variations of the supply voltage. These features are particularly useful for ICs with tough reliability requirements, which are subjected to over-stressing during production tests in order to induce accelerated ageing and thus assess quicker their reliability. This is the case for the High-Temperature Operating Life test, routinely performed on automotive ICs: it implies running the IC at junction temperatures higher than their normal operating range. Obviously, this test cannot be run on an IC that comprises a standard thermal shutdown circuit, not endowed with the features described above.

A fairly straightforward architecture was employed, with the hysteresis implemented by a current source enabled by the output of the circuit. The current source is the key element of the system, its accuracy and sensitivity to supply variations determines the precision the hysteresis width can be set by. Four possible designs were considered for this current source: V_{BE}/R, modified-V_{BE}/R, Widlar and a peaking current source tailored for this circuit. First, a detailed analytical analysis was performed on these sources; it indicated that the modified peaking current source is the best design option for this circuit. Next, sizing equations for this source were derived in order to minimize its sensitivity to temperature and supply variations. Simulation results confirmed the analytical analysis: the chosen current source exhibited a relatively small temperature variation (only 5% over the temperature range 100°C to 180°C) and good insensitivity to the supply variation (its current moved by 5% around the nominal value of 1.25 uA when V_{SUPPLY} varied from 3.5V to 5.5V).

Finally, the proposed circuit was employed to implement the thermal shutdown protection of an integrated LDO for automotive applications. Simulation results and measurements performed on the silicon implementation fully validated the design: the hysteresis width did not change significantly when the activation temperature was varied between 165°C and 185°C and proved to be largely insensitive to supply voltage variations. Thus, the thermal shutdown circuit described here meets the requirements set for it here, typical for automotive applications. Moreover, its performance compare favorably with the performance of similar circuits reported in the open literature.

REFERENCES

[1] Thermal Considerations for Linear Regulators, Application Note ANP2, Sipex Co., Milpitas, 2006, pp. 1-8

[2] G. A. Rincon-Mora, "Analog IC Design with Low-Dropout Voltage Regulators", pp. 347-373, McGraw-Hill Professional, 2009

[3] Y. C. Hung, D. J. Ceng, "A Sub-1V CMOS LDO regulator with multiple protection capabilities", Computer, Consumer and Control (IS3C), 2014, pp. 800-803, doi: 10.1109/IS3C.2014.212

[4] A.-G. Bajenaru, C. Boianceanu, G. Brezeanu, „Investigation of electro-thermal behaviour of a linear voltage regulator and its protection circuits by simulator coupling", International Semiconductor Conf., 2013, pp. 237-240, doi: 10.1109/SMICND.2013.6688665

[5] J. Altet, R. Antonio, "Thermal testing of integrated circuits", pp. 53-96, Kluwer Academic Publisher, 2002

[6] Plesca A, Scintee A, "Thermal aspects related to power assemblies", Advances in Electrical and Computer Engineering, vol. 10, 2010, pp. 23-27, doi: 10.4316/AECE.2010.01004

[7] Zhang B, Feng Q.Y. "A novel thermal-shutdown protection circuit", 3rd International Conference on Anti-Counterfeiting, Security and Identification in Communication (ASID), 2009, pp. 535-538, doi: 10.1109/ICASID.2009.5276996

[8] Nagel, M.H., Fonderie, "Integrated 1V thermal shutdown circuit", Electronics Letters, 1992, vol. 28, pp 969-970, doi: 10.1109/WiPDA.2015.7369293

[9] Tan C., Liu Z., "A bandgap reference and over temperature protection circuit designed for TCXO chip", International Conference on Intelligent Transportation, Big Data & Smart City, 2015, pp. 8-11, doi: 10.1109/ICITBS.2015.257

[10] Tan C., Chen W.,"Design of a Over-Temperature Protection Circuit for Power Management Chip", Journal of Hunan University of Technology, 2009-05

[11] Wu J., Zou X.C.,"An Improved Thermal-Shutdown Circuit with High Precision and Low Power Consumption", Microelectronics & Computer, 2009-02

[12] A. Dutta, S. Alampally, "DFT Implementations for Striking the Right Balance between Test Cost and Test Quality for Automotive SOCs", IEEE International Test Conference, 2008, pp. 1-10, doi: 10.1109/TEST.2008.5483610

[13] B. Peng, I-Y Chen, "IC HTOL Stress Condition Optimization", Defect and Fault Tolerance in VLSI Systems, 19th IEEE International Symposium, 2004, pp 272-279, doi: 10.1109/DFTVS.2004.1347849

[14] Uprating Semiconductors for High-Temperature Applications, TN-00-18, Micron Tehnology Inc., Idaho, 2004, pp. 1-14

[15] P. Brokaw, J. Audy, "Low voltage current mirror and CTAT current source and method ", US5982201 A, 1998

[16] Kerns, D.V., Jr., "Optimization of the peaking current source", Solid-State Circuits, IEEE Journal, 1986, vol. 21, pp. 587-590, doi: 10.1109/JSSC.1986.1052577

[17] Cheng, M.-H., Wu, Z. -W, "Low-power low-voltage reference using peaking current mirror circuit", Electronics Letters, IET, 2015, vol. 41, pp. 572-573, doi: 10.1049/el:20050316